crystals

MDPI

Article

Surface Roughness Effects on Magnetic Properties and Switching Mechanism in Iron Nanowires

Oleksandr Pastukh *, Dominika Kuźma and Piotr Zieliński

Institute of Nuclear Physics Polish Academy of Sciences, PL-31342 Kraków, Poland; dominika.kuzma@ifj.edu.pl (D.K.); piotr.zielinski@ifj.edu.pl (P.Z.)
* Correspondence: oleksandr.pastukh@ifj.edu.pl

Abstract: Nanowires fabricated with experimental techniques are never perfect and possess structural imperfections. The effect of the resulting surface roughness on magnetic properties of iron nanowires has been simulated here with the use of numerical technique involving atomistic-resolved software Vampire. A two-regime or a power-law decrease in the coercive field has been found for the roughness amplitude up to 30% of the perfect radius of the wire. The roughness of the surface of the side face of cylindrical wire makes the ends of the cylinder inequivalent as far as the switching mechanism is concerned. As a result, the switching becomes dominated by a transverse domain wall arising at one specific end only. Both the coercive field and the switching mechanism are essential in designing magnetic devices, e.g., for memory storage.

Keywords: nanowires; atomistic spin model; surface roughness; remagnetization

Citation: Pastukh, O.; Kuźma, D.; Zieliński, P. Surface Roughness Effects on Magnetic Properties and Switching Mechanism in Iron Nanowires. *Crystals* **2023**, *13*, 1617. https://doi.org/10.3390/cryst13121617

Academic Editor: Rajratan Basu

Received: 25 October 2023
Revised: 16 November 2023
Accepted: 20 November 2023
Published: 22 November 2023

1. Introduction

Surface roughness in magnetic nanostructures is critical in defining their magnetic characteristics and performance in a variety of applications. Nanostructures are extremely susceptible to surface impacts due to their small size and high surface area-to-volume ratio. Rough surface in these structures can be both a challenge and an opportunity, depending on the application and surface feature control. In the context of magnetic nanostructures surface roughness can impact their magnetic behavior in several ways: influence magnetic anisotropy [1], affect exchange coupling (especially in multi-layered thin films or core-shell nanostructures) [2], lead to variations in dipolar interactions among neighboring magnetic moments [3], change magnetic reversal by affecting the energy barriers for switching of magnetic moments [4], and reduce or increase the coercive field [5]. Optimizing the performance of magnetic nanostructures in a variety of applications, from medicinal devices and energy harvesting technologies to data storage and sensors, requires an understanding of and ability to control surface roughness.

Elongated ferromagnetic nanostructures (nanostripes, nanowires, nanotubes) showing significant shape anisotropy are intensively studied as candidates for efficient systems capable of storing and processing information [6–8]. Practical realisation of nanodevices on their basis demand stable magnetic configuration and precise control over magnetisation switching process. Due to the size- and shape–dependent interplay between dipolar and exchange interactions the switching in such structures from one stable orientation to another becomes very complex [9–11] even in idealizing models. Therefore, a significant influence on magnetic performance of elongated nanostructures can be exerted by the edge roughness. Probably the first model taking into account such effect in the ferromagnetic thin film was proposed by Bruno [12], who reported a significant contribution of dipolar energy to magnetic anisotropy caused by an interfacial roughness. Later simulations by Gadbois et al. on 1 µm long and 30 nm thick Ni bars showed that rough edges of the bar significantly reduce the switching field [13]. The effect of increased edge roughness on the switching times

and switching fields in permalloy films was also reported by Deak et al. [14]. Experimental investigations of magnetisation reversal in elongated permalloy nanostructures with rough edges were studied by Kirk et al. [15] and Bryan et al. [16]. Both studies showed a strong dependence of the coercive field on the film thickness for different roughness levels of the edges.

The cylindrical ferromagnetic nanowires (NWs) represent an alternative to nanostripes and study of domain walls movement and magnetization switching in these structures opens up new route for nanodevice fabrication. A precise knowledge of such processes is of particular importance in the area of ultra-high-density magnetic recording as well as in giant magnetoresistance (GMR) devices [17]. The controllability and reproducibility of the geometric, chemical, and structural properties of the nanowires depend on the methods of their fabrication. The dominating method is the electrodeposition in porous templates. Arrays of magnetic NWs are usually synthesised using nanoporous templates, such as anodised aluminium oxide (AAO) or polycarbonate [18]. However, no fabrication method is ideal even from the geometric point of view. In most cases, imperfections of the pore walls can cause significant surface roughness of the obtained nanowires and, as a result, alter their magnetic performance [19]. In particular, surface roughness of ferromagnetic nanowires can affect both magnetic switching fields and the corresponding switching patterns [20]. Moreover, as the roughness levels rise, the interaction between domain walls becomes more complex, which is attributed to the asymmetry and dynamic pinning effects [21]. The pronounced deviation from the perfect cylindrical shape of nanowires can promote creation of unconventional magnetic textures with modified dynamics [22,23].

The existing theoretical simulations of surface roughness and its influence on the magnetic properties of material are commonly based on the micromagnetic approach [13–15,21,24]. However, discretization of the material's space into cuboidal cells (with the typical size of a few nanometres) may not always accurately capture the microstructure of the material. Therefore, more detailed and realistic models are needed. Here, we study the effects of edge roughness on the magnetic switching in iron nanowires with diameter of 10 nm, with the use of atomistic spin model simulations. The latter approach gives a possibility to simulate materials with exact crystal structure and microscopic magnetic properties. The influence of such a microscopically resolved surface roughness with different amplitude and distribution along the cylinder on the mean coercive field is studied and the resulting changes in the spin magnetic configuration during remagnetisation are analysed.

2. Geometry of Materials and Calculation Methods

The simulated Fe nanowires have a diameter d = 10 nm and a length l = 100 nm. This gives the aspect ratio of a = 10, which can approximate the properties of real material, since the shape anisotropy, in this case, is close to the one of an infinite cylinder [25]. In the ferromagnetic nanowires, the two different reversal modes are typically observed for the structures with $a \geq 10$, depending on their thickness: transverse domain wall (TDW) mode and the vortex domain wall mode [26]. The considered structures refer to the former case due to their diameter, which is smaller than the critical value for the iron NWs [27]. The simulations performed in this work were based on the atomistic spin model included into Vampire software [28], where the Hamiltonian of the system contains exchange, anisotropy, applied field, and demagnetising field contributions:

$$\mathcal{H} = -\sum_{i \neq j} J_{ij} \mathbf{S}_i \cdot \mathbf{S}_j - \frac{k_c}{2} \sum_i \left(S_x^4 + S_y^4 + S_z^4 \right) - \sum_i \mu_s \mathbf{S}_i \cdot \mathbf{H}_{app} + \mathcal{H}_{demag}. \quad (1)$$

In the above equation, J_{ij} is the Heisenberg exchange, $\mathbf{S}_i$ is a unit vector describing orientation of the local spin moment, k_c is the local cubic anisotropy constant, S_x, S_y, S_z are the corresponding components of the spin moment, μ_s is atomic spin moment, $\mathbf{H}_{app}$ is the external applied field vector. The term $\mathcal{H}_{demag}$ describes the magnetostatic contribution, in the following form $-1/2 \sum_p \mathbf{m}_p^{mc} \cdot \mathbf{H}_{demag}^p$, where $\mathbf{m}_p^{mc}$ is total magnetic moment of

macrocell and $\mathbf{H}^{p}_{demag}$ is demagnetization field. The dipole field calculations were based on the tensor approach, where the dipole tensor is calculated between neighbouring macrocells with atomistic accuracy [29]. The following parameters were applied in calculations: the atomistic spin moment μ_s = 2.22 μ_B, the exchange energy $J_{ij} = 7.05 \times 10^{-21}$ J/link, and the magnetocrystalline anisotropy energy $k_c = 5.65 \times 10^{-25}$ J/atom. The time evolution of the system in the model is described by the Landau-Lifshitz-Gilbert (LLG) equation with Langevin dynamics using the Heun integration scheme [30]:

$$\frac{\partial \mathbf{S}_i}{\partial t} = -\frac{\gamma}{1+\alpha^2}\left[\mathbf{S}_i \times \mathbf{H}^{i}_{eff} + \alpha \mathbf{S}_i \times \left(\mathbf{S}_i \times \mathbf{H}^{i}_{eff}\right)\right], \quad (2)$$

where γ is the gyromagnetic ratio and α is the Gilbert damping parameter, which is taken to be equal to its critical value as suggested by the software for hysteresis loop calculations [31]. $\mathbf{H}_{eff}$ describes the net effective magnetic field on each spin.

The iron nanowire was simulated using bcc crystal structure with a unit cell size of 2.866 Å. In order to introduce a surface roughness the following procedure was applied. First, the cylinder volume was divided into 50 equal cylindrical segments of 2 nm height each, making circular perpendicular cross-sections at every portion of the long axis. Then, for each slice the radius was changed by $\Delta(r)$ from its unperturbed value r. The radius variation was effectuated every 5 deg of circumference with the use of a random number generator with a Gaussian distribution. The width of the Gaussian function, i.e., the standard error describes the depth of the roughness. In what follows we report the results as functions of the percentage of the radius $\Delta(r)/r = 3\sigma$, where σ is the standard deviation of the normal distribution. The approach adopted for the surface roughness implementation in the iron nanowires in the present paper is schematically represented in the Figure 1. Such a method provides a unique surface roughness of each nanowire and can approximate the structure of real materials. In our calculations, six different amplitudes of roughness (5%, 10%, 15%, 20%, 25%, 30%) were applied as depicted in Figure 2. The software Vampire allows one to compute the equilibrium configuration of atomic spins in the whole volume of the so design sample at every strength and direction of the applied magnetic field. The computation of the net magnetization at every value of the magnetic field allowed us to obtain hysteresis loops for every model sample. In addition, the total energy of the system for each roughness amplitude was calculated as a function of external magnetic field.

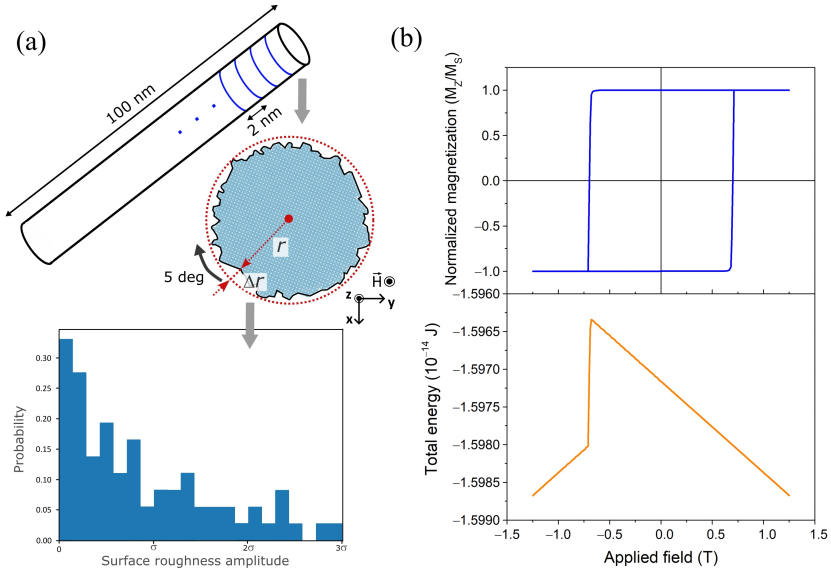

Figure 1. Schematic representation of side face roughness simulation approach (see the text for details) (**a**) and corresponding results obtained in calculations: normalized magnetization and total energy dependence on the applied field (**b**).

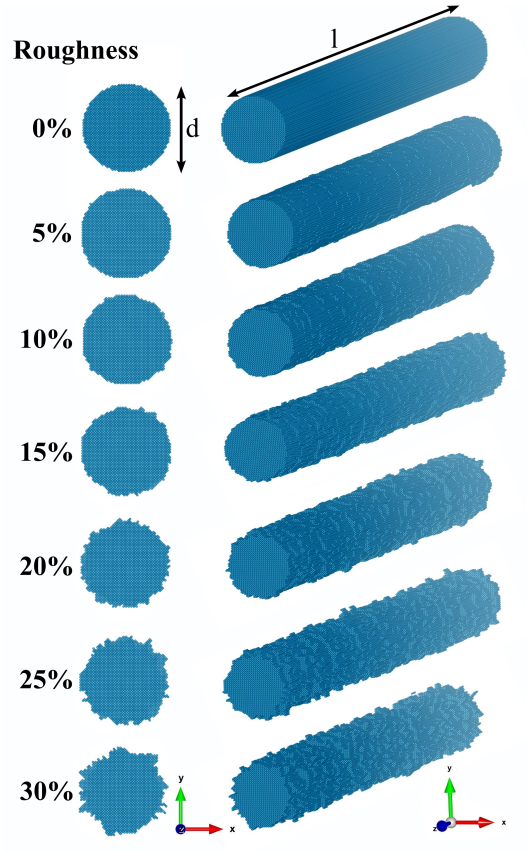

Figure 2. Geometry of investigated nanowires with different surface roughness.

3. Results of Calculations

In order to calculate how the surface roughness affects the magnetic properties of nanowires calculations of hysteresis loop were done for each nanostructure. External field was applied along the long axis of nanowires for all the calculations. The simulations of the field dependent magnetisation were performed for all the structures with different roughness percentage. From the obtained hysteresis loops the coercive field values were calculated. As a result of the applied random distribution, each nanowire has a different surface for each roughness amplitude. This results in a visible distribution of coercivity for each roughness percentage. Therefore, simulations of more than 100 nanostructures with unique edge shapes of each NW were performed. Then, the dependence on the surface roughness was obtained by averaging the coercive field from the set of independent loops for different roughness percentages (Figure 3).

As we can see, the coercive field values have a general trend to decrease with the edge roughness. The two straight lines in Figure 3 correspond to two regimes of the dependence: a weak dependence at $\Delta(r)/r < 20\%$ and a stronger dependence at $\Delta(r)/r > 20\%$. Alternatively, a smooth curve can be fitted to the data. It turns out to involve a non-integer exponent $y = -6.1 \times 10^{-6}(\Delta(r)/r)^{2.6} + 0.72$. The non integer exponent may indicate a self-similar (fractal) nature of the roughness. Small amplitudes of roughness resulted in very slight changes of the surface structure and did not affect significantly the switching field. However, for higher amplitudes, the value of the mean coercivity can decrease up to 10% compared to the value for cylinder with smooth edges. It can be seen also, that the distribution of the coercive field for each roughness percentage increases which explains probably by more significant variations in the surface structure.

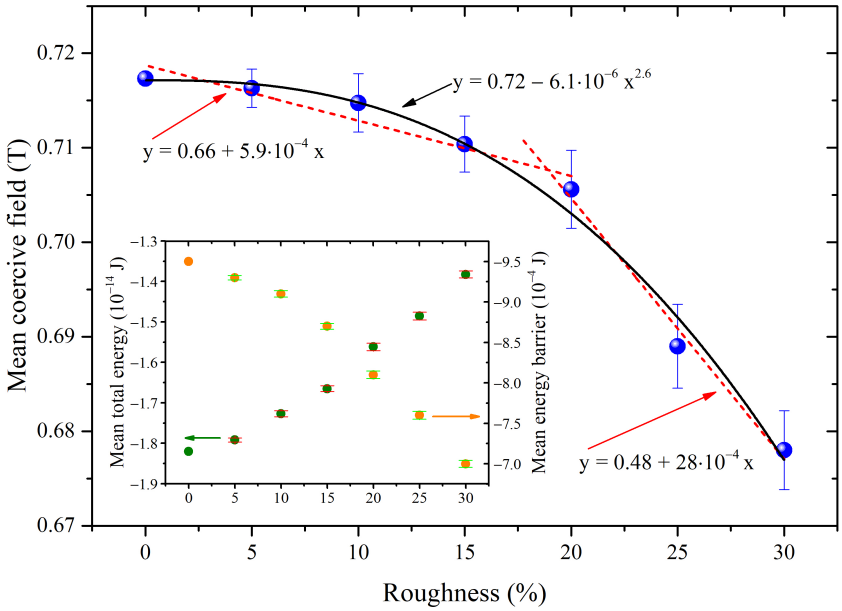

Figure 3. Change of the mean coercive field with the surface roughness increase (inset: change of the total energy and energy barrier with roughness). Dashed lines represent fitting to the linear function and solid line represents fitting to the non-integer exponent. Error bars show the standard deviation of the distribution of the values.

In order to understand the mechanism of change in the coercive field of nanowires with edge roughness we have studied the most important physical quantities involved. The total energy for each applied field value is obtained as an output of simulation and calculated according to the spin Hamiltonian (1). The total energy is the sum of exchange energy of interacting atomic moments, a cubic anisotropy energy, the applied field energy, and magnetostatic energy, which is based on the dipole field calculations. The values of energy in the inset of Figure 3 represent the total energy obtained after applying the saturating field along the long cylinder axis. The values of the energy barrier can be also obtained from the corresponding total energy curves as described in ref [23]. To evaluate the energy barrier that needs to be overcome by the external field in order to initiate switching between two magnetic configurations the difference between the energy value at zero field and at the point where reversal occurs was calculated and presented in the inset of Figure 3. Analysis of change in the mean total energy as a function of the roughness amplitude (the energy values were taken as the average for each roughness percentage) suggests that a rough configuration of cylinder is less energetically favourable as the smooth one. Accordingly, the system tends to switch its magnetisation according to external field direction to reduce the total energy. A tend to faster switch of rough NWs in comparison to smooth also follows from the change of energy barrier between initial magnetic configuration opposite to the actual field and the one along the field. The barrier decreases with increasing roughness (see inset of Figure 3). The main contribution to the total energy for ferromagnetic nanowires is from the exchange and demagnetising field energy. The exchange interaction ensures that the magnetisation remains uniform across all the radial cross-sections of the cylinder along its axis, and depends only on the position along the longest NWs axis. Therefore, significant distortion in the surface structure can only result from change of number of interacting atoms. Interestingly, the total material magnetisation changes significantly despite that. Another factor that affects the switching of magnetic moments from their parallel to antiparallel configuration with respect to the field is the magnetic shape anisotropy, caused by the elongated form of nanowires and originating from magnetostatic (or demagnetisation) energy [32]. A demagnetising field is created, between two opposite magnetic poles of the nanowire. The energy of this stray field is the magnetostatic energy of the system. Since the demagnetising field has a direction

opposite to that of the materials magnetisation, it may an effect on the calculated coercive field. The irregular shape of the nanowire surface plays a key role, since the magnetising force inside the structure placed in a uniform magnetic field is different in magnitude from the applied field and can vary in direction across the NW [33]. Also, deviations from perfect cylindrical geometry of nanowires can cause significant change in the shape anisotropy and provide a reduction in coercive field [34]. We can suppose therefore, that for the increased roughness the magnetostatic field also increases leading to switching of NWs in lower field. Additional aspect that may influence the magnetic behaviour could be spin distortions which may appear at the rough side faces. In the saturation field the smooth as well as the rough faced nanowires have similar spin-states with most of the spins pointed parallel to the long NWs axis. For the case of smooth cylinder, when the switching process starts, the energy is spent on the spin rotation in the bulk as well as at the faces and edges of the structure. However, at the rough faces and edges of NWs, differently oriented distortions from homogeneous or smooth spin-states may occur in switching process. The inhomogeneities consume energy that is the main mechanism of producing noticeable modifications of the net magnetization resulting in changes of the coercive fields as well as shapes of the hysteresis loops [35]. Moreover, we may suppose that such process could also affect the magnetization switching mechanism and would have even much effect for the wider nanostructures [11]. Note, that decrease in the coercive field for the elongated ferromagnets with rough side faces is in agreement with the previous studies [13–15]. Although the nature of such effect in simulated structures can be slightly different, most studies indicate that increasing edge roughness can affect local equilibrium magnetization of the sample and induce the initial formation of reversal modes (i.e., vortices or transverse domain walls).

Another observation can be made when analysing the spin configuration in the structures during remagnetisation process. The employed software enables the retrieval of atomic positions and their spin configurations at a desired stage of the hysteresis loop calculations. A coordinate file is initially produced at the simulation's onset, containing the positions of all the atom in the structure, while the atomic spin files depict a unit vector for each atom and are generated in a series of snapshots throughout the entire simulation. To visualise the spin configuration the POVRay [36] visualisation tool was used. By applying such a procedure the 3D representations of snapshots of the atomic spin moments configuration during magnetization reversal from parallel to antiparallel magnetic moments orientation along the wire axis are shown. Here, two representative cases are considered for the cylinder with the smooth faces and structure with rough edges. The results of the simulations have been visualized by means a colour code provided with the software (Figure 4). The reversal mechanism in NWs with $a \geq 10$ occurs through the formation and propagation of two transverse domain walls, that form at the edges of the cylinder and propagate towards the centre [26]. Initially, the magnetization of the wire is aligned along its long axis. By the reaching of the switching field, two transverse domain walls appear at the wire ends, where the demagnetizing field has its strongest value. By propagating towards each other they separate the central domain from two outer domains. This central domain is oriented in the opposite direction to the external field. Finally, the two TDW collide with each other and annihilate leading to the reversal of the whole cylinder in the direction of applied field. Such a scenario is observed for the simulated nanowire with the smooth edges (Figure 4a). However, the switching mechanism changes as the rough edges are introduced into the structure. Transverse domain walls do not form simultaneously at both ends of NW but proceed from one end or the other with, visibly, no communication between end states (Figure 4b). Such behaviour is in agreement with the experimental observations and typical for the real materials, which possess structural imperfections of the surface [37]. Since the reversal of a NW starts with the nucleation of a transverse domain wall at its ends, we may suppose also, that a random distribution of rough edges produces an inequivalence of both ends of the NW. As a result, the magnetization near the ends of the nanowire becomes inhomogeneous. Then, when

the critical reverse field is reached (i.e., coercive field), only one end becomes preferential for forming a reversal mode and the transverse domain wall proceeds rapidly through the whole nanowire.

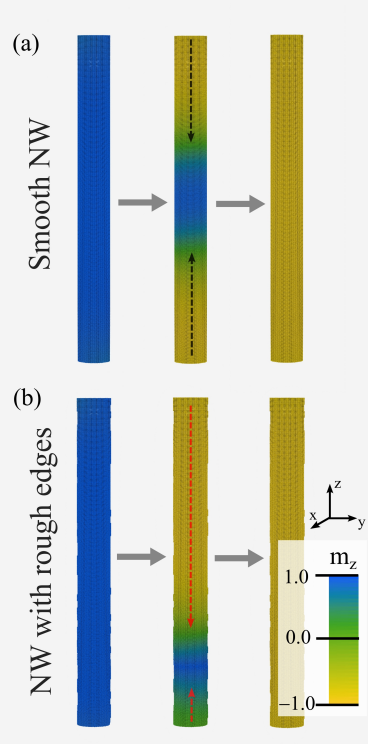

Figure 4. Spin magnetic configuration of NW during remagnetization process for the case of smooth nanowire (**a**) and NW with rough edges (**b**). The color changes with the spin projection as shown in the inserted bar. The boundary cases correspond to pure blue and pure yellow colors for the spins aligned up and down, along the NW axis.

As it is known, NWs can be fabricated by various synthesis methods (e.g., electrodeposition, lithographic patterning, etc.). Nevertheless, the fabrication strategies do not give the possibility to obtain perfect geometrical shape and smooth surface of nanostructures [20,38,39], since surface roughness cannot be fully avoided and may influence the magnetic behavior. Most of experimental studies of the ferromagnetic nanowires which take into account such effects, however, concentrate on the ferromagnetic domain walls' internal structure, in relation to the cylinders' irregular or rough surfaces. Our study, in contrast, gives important quantitative analysis of the impact of surface roughness with different amplitude on the magnetic properties in magnetic NWs. Nevertheless, simulated magnetic behavior of iron NWs can be qualitatively compared with experimental observations. For example, a decrease in switching field was found in the NiFe rectangular nanowires with rough edges [15], which explains by the initial nucleation of reversal modes at the structural defects. Similar effect was also observed in Ni NWs, where the initiation of magnetization reversal was caused by significant geometric irregularities in nanowires [40]. Based on our simulations we may conclude that in real materials, an increased edge roughness can have an impact on the sample's local equilibrium magnetization causing an initiation of the reversal process and, by this, produce a decrease in the coercive field. This can be seen in Figure 3. As we have shown in the simulations, an important role in switching may be also played by a change in the TDWs formation in the NWs and way of their propagation. Similar effect may be found in experimental observations. Study of electrodeposited permalloy nanowires shows that microstructural defects cause that two sides of NW may switch at different fields [41]. Magnetic behavior studies of elongated permalloy and Co nanostructures show that when the ends of particle are asymmetrical the

nucleation starts at only one of the ends and DW propagates then along the long axis of the structure [37], which is similar to the structures observed in simulations of rough surfaces (see Figure 4b). Experimental study of permalloy nanowires show that edge roughness may also affect the TDW degree of asymmetry, which may alter along the nanowire, as the result of different local spin configurations at the rough edges [39,42].

The motion of domain walls in thin ferromagnetic nanowires is the subject of great interest, gaining from the diverse range of potential applications, including logic-, sensing-, or information storage units. Many of these applications rely on the presence of multiple domain walls, with the possibility of their independent management and repositioning [43]. Therefore our study shows an important role of surface roughness in the domain walls motion, which should be taken into consideration during designing and fabrication of magnetic nanowire-based devices.

4. Conclusions

The simulations of surface roughness effect on the field dependent magnetisation in iron nanowires have been performed with the use of atomistic spin model. Small change in the surface structure does not modify much the calculated coercive field. However, more significant modification of the nanowire surface can result in a more pronounced decrease in switching field up to 10%. Thus, two regimes of variation of the coercive field: a weak up to 20% of roughness and strong for $\Delta(r)/r > 20\%$. Alternatively, the coercive field dependence can be fitted with a function showing a non-integer power, which may witness to a self-similar or fractal behaviour of the roughness [44]. The variation of the coercive field is entailed by modifications of the exchange interactions and of demagnetising field. Analysis of the spin configuration during cylinders' remagnetisation reveals change in the transverse domain walls propagation. Propagation of two TDW becomes non-simultaneous from both NW ends at the rough edge structure in comparison with smooth surface. The performed calculations preset a preliminary results of surface roughness influence on the magnetic properties of iron nanowires. Further research can be devoted to more complex structures or nanowires with higher diameter, where the vortex domain walls appears or domain wall pinning can be observed. Of particular interest also could be simulations of arrays of such nanostructures, where the long-range dipolar interactions between magnetic elements play important role. We can suppose, that surface roughness in such structures will have more significant influence on the magnetic properties and probably reveal new interesting effects. Of special interest is the fact that making the surface rough enough makes the apparently similar ends of cylinders practically inequivalent in the switching mechanism, that may be beneficial in designing memory storage or analogous devices.

Author Contributions: Conceptualization, O.P.; methodology, O.P.; software, O.P. and D.K.; investigation, O.P. and D.K.; validation, D.K. and P.Z.; writing—original draft preparation, O.P.; writing—review and editing, D.K. and P.Z.; visualization, O.P. and D.K.; supervision, P.Z. All authors have read and agreed to the published version of the manuscript.

Funding: The numerical calculations were performed at Poznan Supercomputing and Networking Center (Grant No. 630).

Data Availability Statement: Data is contained within the article.

Acknowledgments: We thank Richard F L Evans and the VAMPIRE team from the University of York for an instructive course of the software https://vampire.york.ac.uk/ (accessed on 4 September 2023).

Conflicts of Interest: The authors declare no conflict of interest.

References

1. Chang, C.R. Influence of roughness on magnetic surface anisotropy in ultrathin films. *J. Appl. Phys.* **1992**, *72*, 596–600. [CrossRef]
2. Desai, M.; Misra, A.; Doyle, W. Effect of interface roughness on exchange coupling in synthetic antiferromagnetic multilayers. *IEEE Trans. Magn.* **2005**, *41*, 3151–3153. [CrossRef]

3. Altbir, D.; Kiwi, M.; Ramírez, R.; Schuller, I.K. Dipolar interaction and its interplay with interface roughness. *J. Magn. Magn. Mater.* **1995**, *149*, L246–L250. [CrossRef]
4. Meyners, D.; Brückl, H.; Reiss, G. Influence of boundary roughness on the magnetization reversal in submicron sized magnetic tunnel junctions. *J. Appl. Phys.* **2003**, *93*, 2676–2680. [CrossRef]
5. Dantas, A.L.; Rebouças, G.; Silva, A.S.; Carriço, A.D.S. Interface roughness effects on coercivity and exchange bias. *J. Appl. Phys.* **2005**, *97*, 10K105 . [CrossRef]
6. Walter, E.; Ng, K.; Zach, M.; Penner, R.; Favier, F. Electronic devices from electrodeposited metal nanowires. *Microelectron. Eng.* **2002**, *61*, 555–561. [CrossRef]
7. Ding, J.; Kostylev, M.; Adeyeye, A. Realization of a mesoscopic reprogrammable magnetic logic based on a nanoscale reconfigurable magnonic crystal. *Appl. Phys. Lett.* **2012**, *100*, 073114 . [CrossRef]
8. Kent, A.D.; Worledge, D.C. A new spin on magnetic memories. *Nat. Nanotechnol.* **2015**, *10*, 187–191. [CrossRef]
9. Gadbois, J.; Zhu, J.G.; Vavra, W.; Hurst, A. The effect of end and edge shape on the performance of pseudo-spin valve memories. *IEEE Trans. Magn.* **1998**, *34*, 1066–1068. [CrossRef]
10. Sun, L.; Hao, Y.; Chien, C.L.; Searson, P.C. Tuning the properties of magnetic nanowires. *IBM J. Res. Dev.* **2005**, *49*, 79–102. [CrossRef]
11. Kuźma, D.; Laskowski, Ł.; Kłos, J.W.; Zieliński, P. Effects of shape on magnetization switching in systems of magnetic elongated nanoparticles. *J. Magn. Magn. Mater.* **2022**, *545*, 168685. [CrossRef]
12. Bruno, P. Dipolar magnetic surface anisotropy in ferromagnetic thin films with interfacial roughness. *J. Appl. Phys.* **1988**, *64*, 3153–3156. [CrossRef]
13. Gadbois, J.; Zhu, J.G. Effect of edge roughness in nano-scale magnetic bar switching. *IEEE Trans. Magn.* **1995**, *31*, 3802–3804. [CrossRef]
14. Deak, J.; Koch, R. The effect of edge roughness on magnetization reversal in micron-sized permalloy thin films. *J. Magn. Magn. Mater.* **2000**, *213*, 25–31. [CrossRef]
15. Kirk, K.; Scheinfein, M.; Chapman, J.; McVitie, S.; Gillies, M.; Ward, B.; Tennant, J. Role of vortices in magnetization reversal of rectangular NiFe elements. *J. Phys. D Appl. Phys.* **2001**, *34*, 160. [CrossRef]
16. Bryan, M.; Atkinson, D.; Cowburn, R. Experimental study of the influence of edge roughness on magnetization switching in Permalloy nanostructures. *Appl. Phys. Lett.* **2004**, *85*, 3510–3512. [CrossRef]
17. Fert, A.; Piraux, L. Magnetic nanowires. *J. Magn. Magn. Mater.* **1999**, *200*, 338–358. [CrossRef]
18. Kac, M.; Mis, A.; Dubiel, B.; Kowalski, K.; Zarzycki, A.; Dobosz, I. Template-Assisted Iron Nanowire Formation at Different Electrolyte Temperatures. *Materials* **2021**, *14*, 4080. [CrossRef]
19. Cornelius, T.; Schiedt, B.; Severin, D.; Pépy, G.; Toulemonde, M.; Apel, P.Y.; Boesecke, P.; Trautmann, C. Nanopores in track-etched polymer membranes characterized by small-angle x-ray scattering. *Nanotechnology* **2010**, *21*, 155702. [CrossRef]
20. Biziere, N.; Gatel, C.; Lassalle-Balier, R.; Clochard, M.C.; Wegrowe, J.E.; Snoeck, E. Imaging the fine structure of a magnetic domain wall in a Ni nanocylinder. *Nano Lett.* **2013**, *13*, 2053–2057. [CrossRef]
21. Dolocan, V.O. Domain wall pinning and interaction in rough cylindrical nanowires. *Appl. Phys. Lett.* **2014**, *105*, 162401 . [CrossRef]
22. Burn, D.M.; Arac, E.; Atkinson, D. Magnetization switching and domain-wall propagation behavior in edge-modulated ferromagnetic nanowire structures. *Phys. Rev. B* **2013**, *88*, 104422. [CrossRef]
23. Sáez, G.; Díaz, P.; Cisternas, E.; Vogel, E.E.; Escrig, J. Information storage in permalloy modulated magnetic nanowires. *Sci. Rep.* **2021**, *11*, 20811. [CrossRef] [PubMed]
24. Vatansever, E.; Yüksel, Y. Nonmagnetic impurities and roughness effects on the finite temperature magnetic properties of core–shell spherical nanoparticles with antiferromagnetic interface coupling. *J. Magn. Magn. Mater.* **2017**, *441*, 548–556. [CrossRef]
25. Sellmyer, D.; Zheng, M.; Skomski, R. Magnetism of Fe, Co and Ni nanowires in self-assembled arrays. *J. Phys. Condens. Matter* **2001**, *13*, R433. [CrossRef]
26. Proenca, M.P.; Rial, J.; Araujo, J.P.; Sousa, C.T. Magnetic reversal modes in cylindrical nanostructures: From disks to wires. *Sci. Rep.* **2021**, *11*, 10100. [CrossRef] [PubMed]
27. Abo, G.S.; Hong, Y.K.; Park, J.; Lee, J.; Lee, W.; Choi, B.C. Definition of magnetic exchange length. *IEEE Trans. Magn.* **2013**, *49*, 4937–4939. [CrossRef]
28. Evans, R.F.; Fan, W.J.; Chureemart, P.; Ostler, T.A.; Ellis, M.O.; Chantrell, R.W. Atomistic spin model simulations of magnetic nanomaterials. *J. Phys. Condens. Matter* **2014**, *26*, 103202. [CrossRef]
29. Meo, A. Atomistic Model of Magnetisation Dynamics and Equilibrium Properties of Magnetic Tunnel Junctions. Ph.D. Thesis, University of York, Heslington, UK, 2018.
30. García-Palacios, J.L.; Lázaro, F.J. Langevin-dynamics study of the dynamical properties of small magnetic particles. *Phys. Rev. B* **1998**, *58*, 14937. [CrossRef]
31. Meo, A.; Chureemart, P.; Wang, S.; Chepulskyy, R.; Apalkov, D.; Chantrell, R.W.; Evans, R.F. Thermally nucleated magnetic reversal in CoFeB/MgO nanodots. *Sci. Rep.* **2017**, *7*, 16729. [CrossRef]
32. Mørup, S.; Frandsen, C.; Hansen, M.F. Magnetic properties of nanoparticles. In *The Oxford Handbook of Nanoscience and Technology*; Oxford University Press: Oxford, UK, 2010; Volume 2, pp. 713–744.
33. Osborn, J.A. Demagnetizing factors of the general ellipsoid. *Phys. Rev.* **1945**, *67*, 351. [CrossRef]

34. Ott, F.; Maurer, T.; Chaboussant, G.; Soumare, Y.; Piquemal, J.Y.; Viau, G. Effects of the shape of elongated magnetic particles on the coercive field. *J. Appl. Phys.* **2009**, *105*. [CrossRef]
35. Bryan , M.; Atkinson, D.; Cowburn, R. Edge roughness and coercivity in magnetic nanostructures. *J. Phys. Conf. Ser.* **2005**, *17*, 40. [CrossRef]
36. Persistence of Vision Pty. Ltd. Version 3.6, 2004. Available online: http://www.povray.org (accessed on 18 September 2023).
37. Ruhrig, M.; Khamsehpour, B.; Kirk, K.; Chapman, J.; Aitchison, P.; McVitie, S.; Wilkinson, C. The fabrication and magnetic properties of acicular magnetic nano-elements. *IEEE Trans. Magn.* **1996**, *32*, 4452–4457. [CrossRef]
38. Tang, S.; Vongehr, S.; Ren, H.; Meng, X. Diameter-controlled synthesis of polycrystalline nickel nanowires and their size dependent magnetic properties. *CrystEngComm* **2012**, *14*, 7209–7216. [CrossRef]
39. Hoang, D.Q.; Tran, M.T.; Cao, X.H. The effect of edge-roughness of magnetic nanowires on the degree of asymmetry in transverse domain walls. *RSC Adv.* **2017**, *7*, 49188–49193. [CrossRef]
40. Pitzschel, K.; Bachmann, J.; Martens, S.; Montero-Moreno, J.M.; Kimling, J.; Meier, G.; Escrig, J.; Nielsch, K.; Görlitz, D. Magnetic reversal of cylindrical nickel nanowires with modulated diameters. *J. Appl. Phys.* **2011**, *109*, 033907 . [CrossRef]
41. Sokolov, A.; Sabirianov, R.; Wernsdorfer, W.; Doudin, B. Magnetization reversal of individual nanowires with controlled defects. *J. Appl. Phys.* **2002**, *91*, 7059–7061. [CrossRef]
42. Hoang, D.Q.; Cao, X.H. Edge defects inducing asymmetric transverse domain walls created in Ni80Fe20 nanowires. *J. Phys. D Appl. Phys.* **2021**, *55*, 075002. [CrossRef]
43. Toscano, D.; Ferreira, V.; Leonel, S.; Coura, P.; Sato, F.; Dias, R.; Costa, B. Position of the transverse domain wall controlled by magnetic impurities in rectangular magnetic nanowires. *J. Appl. Phys.* **2014**, *115*, 163906 . [CrossRef]
44. Brown, J.H.; Gupta, V.K.; Li, B.L.; Milne, B.T.; Restrepo, C.; West, G.B. The fractal nature of nature: Power laws, ecological complexity and biodiversity. *Philos. Trans. R. Soc. Lond. Ser. B Biol. Sci.* **2002**, *357*, 619–626. [CrossRef] [PubMed]